Electronic Supplementary Material (ESI) for Sustainable Energy & Fuels.

An Open-Source Platform for 3D-Printed Redox Flow Battery Test Cells (Supplementary Information)

Hugh O'Connor[a]; Josh J. Bailey[a,b,c]; Oana M. Istrate[b]; Peter A.A. Klusener[d]; Rob Watson[b]; Stephen Glover[b]; Francesco Iacoviello[c]; Dan J.L. Brett[c]; Paul R. Shearing[c]; Peter Nockemann[a*]

a. The QUILL Research Centre, School of Chemistry and Chemical Engineering, Queen's University Belfast, David Keir Building, 39-123 Stranmillis Rd, Belfast BT9 5AG

b. School of Mechanical and Aerospace Engineering, Queen's University Belfast, Ashby Building, Stranmillis Rd, Belfast BT9 5AG

c. Electrochemical Innovation Laboratory, Department of Chemical Engineering, University College London, WC1E 7JE, United Kingdom

d. Shell Global Solutions International B.V., Grasweg 31, 1031 HW Amsterdam, The Netherlands.

*Corresponding author

Typical flow battery test cells from literature

To ensure the cell designed was evaluated under conditions that are representative of those examined in literature, the details of several flow-through test cells used by other researchers have been collated. Although the duration, dimensions and flow rate are not typically the most crucial parameters investigated in literature, they are vital in evaluating the test cell detailed in this work.

Table S1. Flow through test cells from literature, with a number of key parameters for test cell design

Cell no.	Reference	Description	Cell Dimensions (mm)	Longest reported test duration	Highest reported electrolyte flow rate (mL min^{-1})	Applied current density (mA cm^{-1})	Energy Efficiency (%)
1	Sun *et al.*[1]	SLA 3D-printed, bolted around exterior	~22.5 x 22.5	~130 hours	40	40	45.2
2	Ghimire *et al.*[2]	PVC flow frames, machined. Flow plate closed with gasket	100 x 100	~60 hours	100	40-80	~72.5-88
3	Davies *et al.*[3]	Polyolefin gaskets, with inlets and outlets machined into graphite blocks	50 x 62	~72 hours	200	90-435	69.5-27.1
4	Vrána *et al.*[4]	Commercial cell (Pinflow energy storage) PVC flow plates, clamped around exterior	40 x 50	500 cycles ~500 hours**	50	50-200	~57.5-85
5	Mazúr *et al.*[5]	PVC flow plates, graphite composite plates	40 x 50	3 cycles ~14 hours**	40	50-150	~49.5-85
6	Armstrong *et al.*[6]	SLA 3D-printed, VeroWhite. Threaded fittings with lathe. Clamped around perimeter	40 x 20	~13 hours	60	0.125*	44.1*
7	Chen et al.[7, 8] Knehr *et al.*[9]	PVDF endplates and spacers	100 x 100	~102 hours	20	20-80 20-80	60-90 80-95
8	Zhang *et al.*[10]	Acrylic flow channels, silica gaskets, clamped around exterior	~22.5 x 22.5	10 cycles ~25 hours**	50	40	~84.8**
9	Leung *et al.*[11]	Acrylic flow channels, silicone gaskets, clamped around exterior	50 x 70	~53 hours	180	40	73
10	Kim *et al*.[12] Li *et al.*[13] Wang *et al.*[14] Wei *et al.*[15] Li *et al.*[16]	Grooves machined into graphite current collector, sealed with PTFE gaskets	20 x 50	100 cycles ~320 hours**	20	50 25-100 50* 50 50-150	83.7 83-88 82* 81 ~67.5-90
11	Jiang *et al.*[17] Li *et al.*[18] Wenjing *et al.*[19] Li *et al.*[20]	Plastic flow plates, bolted around exterior, graphite bipolar plat/ current collectors	50 x 50	200 cycles ~350 hours**	60	40-120 40-200 40-200 40-80	~40-85 ~65-87.5 ~65-90 ~77.5-88.1
12	Roe *et al.*[21]	PVC flow frames, glassy carbon electrode collector	50 x 45	90 cycles ~390 hours**	-	50-80	75
13	Janoschka *et al.*[22, 23]	Commercial Cell (Jenna batteries) PTFE flow frames, EPDM gaskets and graphite and nickel current collectors	22.5 x 22.5	100 cycles ~85 hours**	20	40* 50-200*	75-80* ~40-75*
14	This work (3D-printed cell)	3D-printed ABS cell body and manifolds, central clamp, graphite/ brass current collectors	50 x 50	Electrochemical tests; 100 hours Leak test; 744 hours	50	50	81.4
15	This work (commercial cell)	Commercial cell (C-tech innovation), CNC-machined PVC flow plates, stainless steel endplates, clamped around exterior and centrally	50 x 50	20 hours	50	50	78

* not an all-vanadium system ** calculated ***leak test

Chemical compatibility testing

The specimens used for the chemical compatibility testing (shown in Figure S1) consisted of a cylinder with a diameter of 15 mm and a height of 30 mm. Each specimen had a 5 mm diameter hole with a depth of 20 mm and took ~1 hour to print, depending on the recommended print speed.

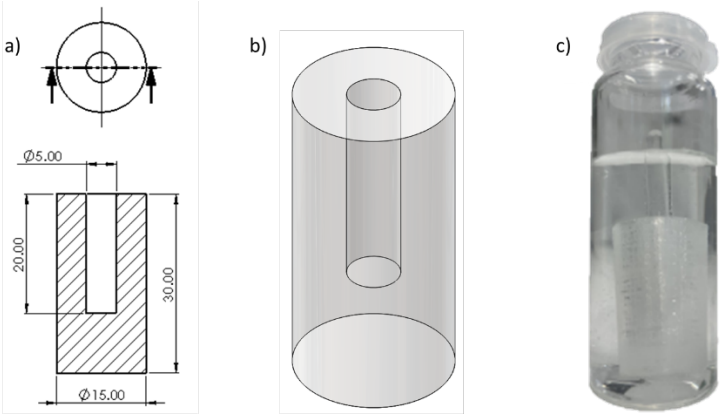

Figure S1. The 3D-printed samples used during compatibility testing. (a) Detailed drawing of specimen showing a cross-section through the centre, (b) 3D-model of the specimen. (c) PP specimen sample bottle during compatibility test, held in solution using a 4 mm diameter glass rod.

These specimens were then tested in ten solutions, which could potentially be used in redox flow batteries. 3 M sulfuric acid (H_2SO_4) was prepared using deionized water (diH_2O) and concentrated H_2SO_4 (99.99 wt.%, Alfa Aesar). 1 M potassium hydroxide (KOH) was prepared by dissolving flakes of KOH (reagent grade, 90%, Sigma-Aldrich) in diH_2O using a magnetic stirrer. The 2 M sodium chloride (NaCl) was prepared by dissolving NaCl crystals (≥99.0%, Sigma-Aldric) in diH_20 using a magnetic stirrer. 3 M hydrochloric acid (HCl) was prepared from concentrated HCL (37wt.%, Alfa Aesar) and diH_20 using a magnetic stirrer. Similarly, 3 M methanesulfonic acid (MSA)) was prepared from concentrated MSA (98+ wt.%, Alfa Aesar) and diH_2O. For the non-aqueous solutions, acetonitrile (anhydrous, 99.8%, Sigma-Aldrich) was used as received, as was propylene carbonate (anhydrous, 99.7%, Sigma Aldrich) and dichloromethane (99+%, Alfa Aesar). The ionic liquid, [$P_{666\,14}$] [NTf_2], trihexyl tetradecyl phosphonium bistriflimide) was prepared by adding trihexyltetradecylphosphonium chloride (10 g, 19.3 mmol) to a round bottom flask in dichloromethane (50 mL) followed by lithium bistrifluoromethanesulfonimidate (16.6 g, 57.8 mmol) in deionised water (50 mL). The reaction was stirred at room temperature for 24 h. The organic layer was washed with deionised water (3 × 50 mL), dried over magnesium sulfate and concentrated to give a viscous yellow liquid.

Electrochemical-CFD model

Simulations were carried out using COMSOL Multiphysics 5.6 with the electrochemistry and CFD add-ons. The simulations shown in Figure 4 of the main text used ~150,000 tetrahedral elements. The interfaces used were the "free and porous media flow" and the "tertiary current distribution, Nernst-Plank" modules. The model used examines flow through the negative half-cell of a flow battery in 3D and was developed by Ma *et al.*[24], based on an approach for modelling vanadium flow batteries developed by Shah *et al.*[25] and later simplified by You *et al.*[26] This model has also been employed by Gurieff *et al.*[27] to examine novel flow cell topologies. The parameters used are summarised in Table S1.

Table S2. CFD-Electrochemical Model Parameters

Parameter	Symbol	Value	Unit
Inlet Area	A	7.07	mm^2
Anodic transfer coefficient: negative	$\propto_a$	0.5	
Cathodic transfer coefficient: positive	$\propto_c$	0.5	
Initial Vanadium Concentration	c^0	1500	mol m^{-3}
Carbon Fibre Diameter	d_f	1.76×10^{-5}	m
V^{2+}/ V^{3+} Diffusion Coefficient	D_i	2.40E-06	cm^2 s^{-1}
Nernst Potential	E_0	-0.255	V
Porous Electrode Porosity	ε	0.929	
Applied Current Density	I	50	mA cm^{-2}
Negative standard reaction rate constant	k_c	1.70×10^{-7}	m s^{-1}
Kozeny-Carman constant	K_{CK}	4.28	
Electrolyte Viscosity	μ	4.93×10^{-3}	Pa s
Outlet Pressure	p	0	Pa
Inlet Volumetric Flow Rate	Q	25	ml min^{-1}
Electrolyte Density	ρ	1208.40	kg m^{-3}
Porous Electrode Conductivity	σ_s	1000	S m^{-1}
State of Charge	SOC	50	%
Porous Electrode Specific Surface Area	a	162	m^{-1}
Temperature	T	298	K

X-ray CT scanning

A summary of the X-ray computed tomography results can be seen in Table S2, along with vanadium deposits for k-values of 0.90, 1.00, and 1.05 in ABS samples in Figure S2.

Table S3. Summary of the X-ray computed tomography results

Sample	PP			ABS		
Flow rate	0.90	1.00	1.05	0.90	1.00	1.05
Porosity	1.90%	0.35%	0.07%	6.41%	3.61%	1.59%
Vanadium content	Negligible			0.42%	0.11%	0.03%

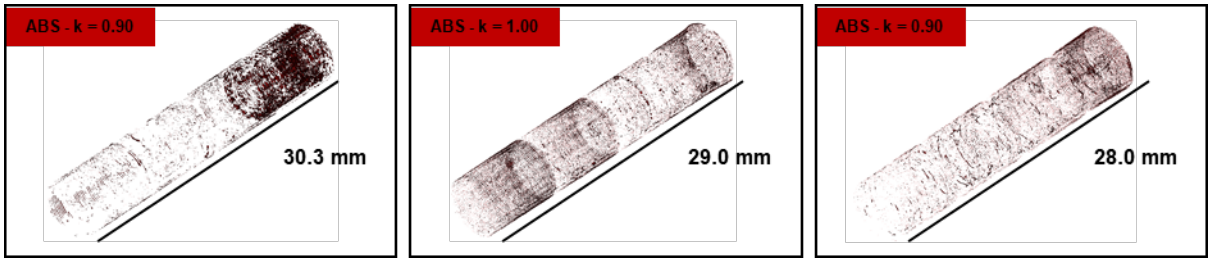

Figure S2. Vanadium deposits for k-values of 0.90, 1.00, and 1.05 in ABS samples

Unoptimised vs Optimised Design

The cell designs detailed in the “Test cell design” section, can be seen in Figure S3. In Figure S3a, the overall footprint of the cell in which both manifold designs and the sealing structure are contained can be seen. The two manifolds different manifold designs can be seen in Figures S3b-e.

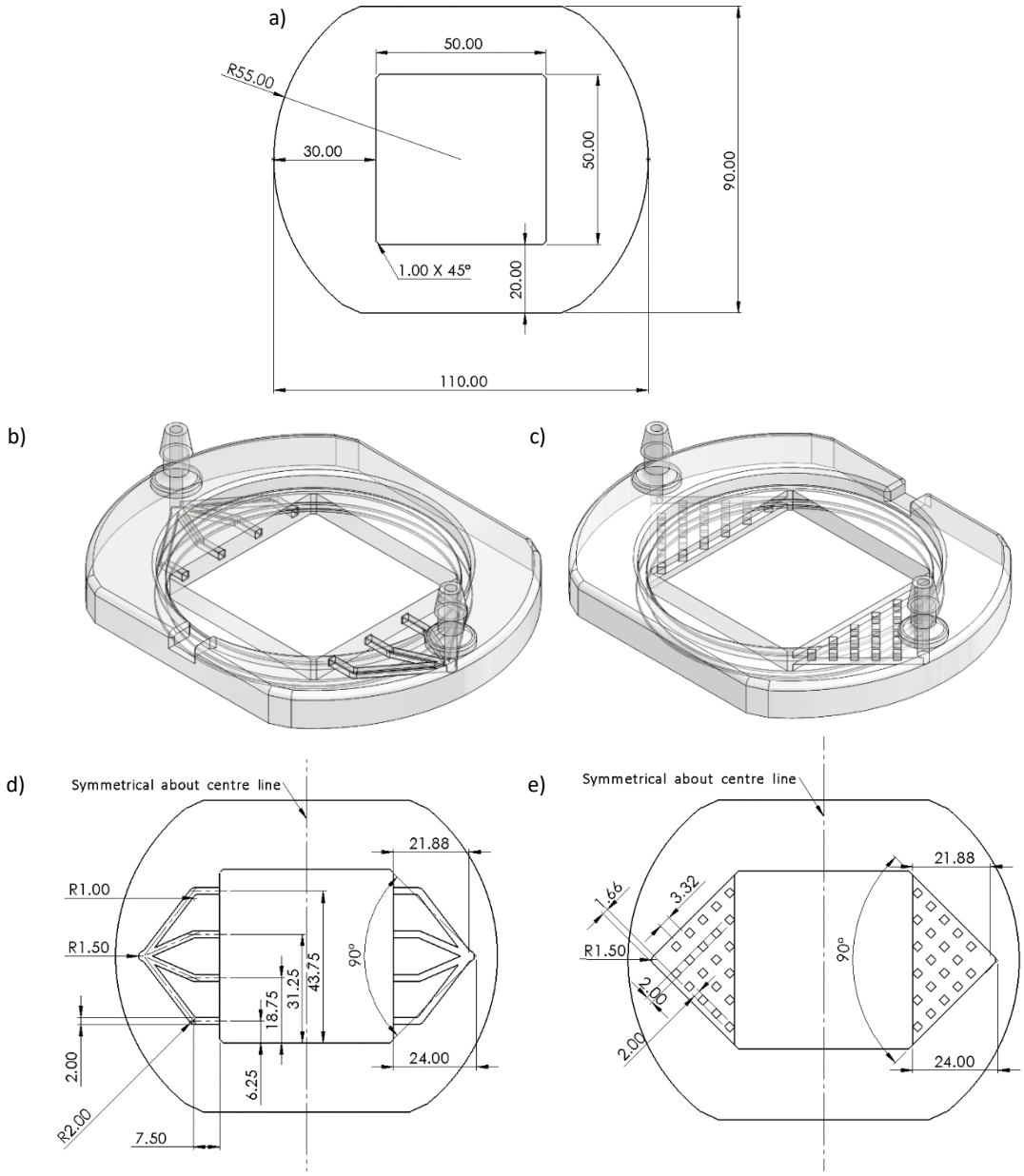

Figure S3. Cell design schematics and drawings. (a) Drawing showing cell footprint, within which both manifold designs were contained. (b) Schematic of cell with unoptimised manifold design. (c) Schematic of cell with optimised manifold design. (d) Drawing showing dimensions of unoptimised manifold design. (e) Drawing showing dimensions of optimised manifold design.

Cell assembly guide

Prior to assembly, the gasket shape is traced using the half-cell as a template. The gaskets were then cut to size using scissors. The assembly steps in Figure S4 were then followed.

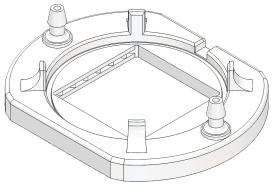

Step 1. Place half-cell on flat surface

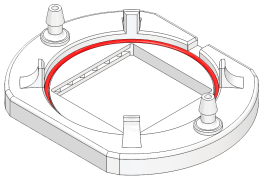

Step 2. Insert O-ring into groove

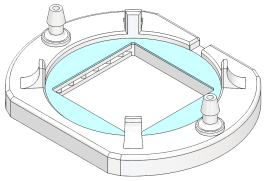

Step 3. Insert gasket into groove

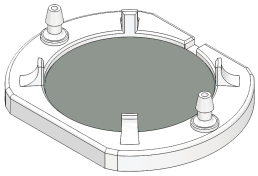

Step 4. Place graphite disk on top of O-ring

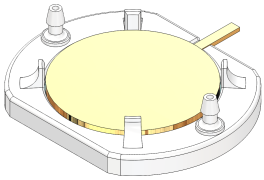

Step 5. Place current collector on top of graphite disk

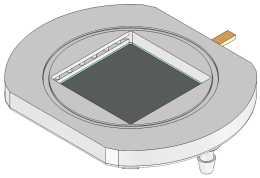

Step 6. Flip cell current collector side facing down. Optional: place current collector on a raised surface to provide clearance for nozzles

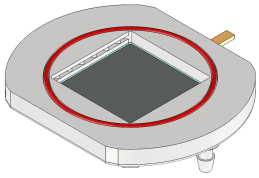

Step 7. Insert O-ring into groove

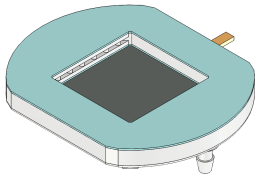

Step 8. Place gasket on top of O-ring. Optional: to hold gasket in place during the remainder of the assembly process, place small strips of adhesive tape below inlet and outlet

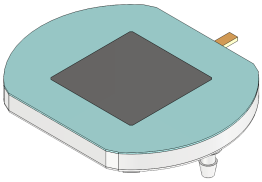

Step 9. Place electrode into electrode compartment

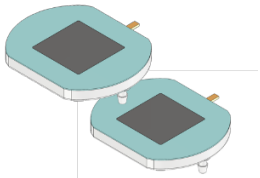

Step 10. Repeat Steps 1-9 for the second half-cell

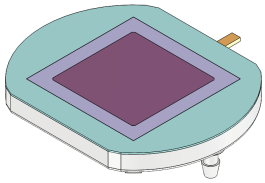

Step 11. Position membrane on one half-cell

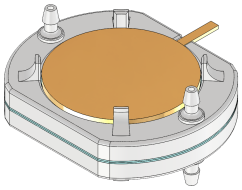

Step 12. Whilst holding components in place, lower one half-cell on top of the other

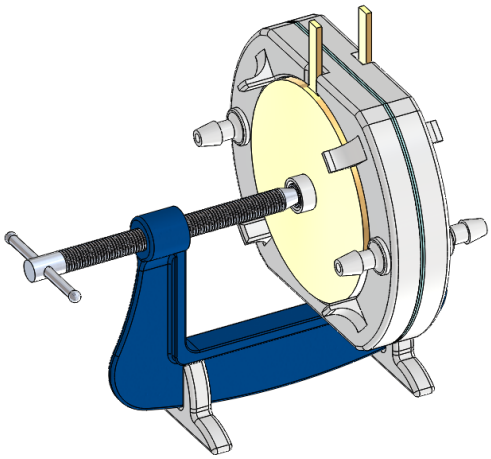

Step 13. Place cell in clamp with current collector tabs facing upwards. Hand tighten clamp then adjust to 8 Nm using torque wrench

Figure S4. Cell assembly guide

The fully assembled cell was then leak-tested with diH_2O prior to use with electrolyte during charge-discharge testing.

Build Plate Adhesion

Along with the methods described in the main text, a number of other methods to ensure good build plate adhesion with 3D-printed parts were employed throughout this work. These included a thin layer of PVA glue[28] as well as an adhesive spray (Dimafix) for ABS and PP tape for PP[29]. The removal of this adhesive/ the brim (if used) represents the only post-processing required during the printing process. All filaments used in this work are available in both 2.85 mm and 1.75 mm diameters, which are the most commonly used filament diameters for FDM printing.

Charge-discharge testing

Equations 1-3 (Ma *et al.*[30]) were used to calculate the coulombic, voltage and energy efficiencies of the cells in the "Charge-discharge testing" section.

$$Coulombic\ efficiency\ (\%) = \frac{Discharge\ capacity\ (mAh)}{Charge\ capacity\ (mAh)} \times 100 \quad (1)$$

$$Voltage\ efficiency\ (\%) = \frac{Average\ discharge\ voltage\ (V)}{Average\ charge\ voltage\ (V)} \times 100 \quad (2)$$

$$Energy\ efficiency\ (\%) = \frac{Discharge\ energy\ (Wh)}{Charge\ energy\ (Wh)} \times 100 \quad (3)$$

The effect of reduced pumping speed (from 50 mL min^{-1} to 25 mL min^{-1}) can be seen in Figure S5, exhibiting a similar performance increase to that observed between the unoptimised and optimised manifold designs. A reduction in coulombic efficiency is also observed in Figures S5a and b, from 96.1% to 91.2% as the flow rate increases from 25 to 50 mL min^{-1}. This behaviour has also been observed elsewhere in literature[31].

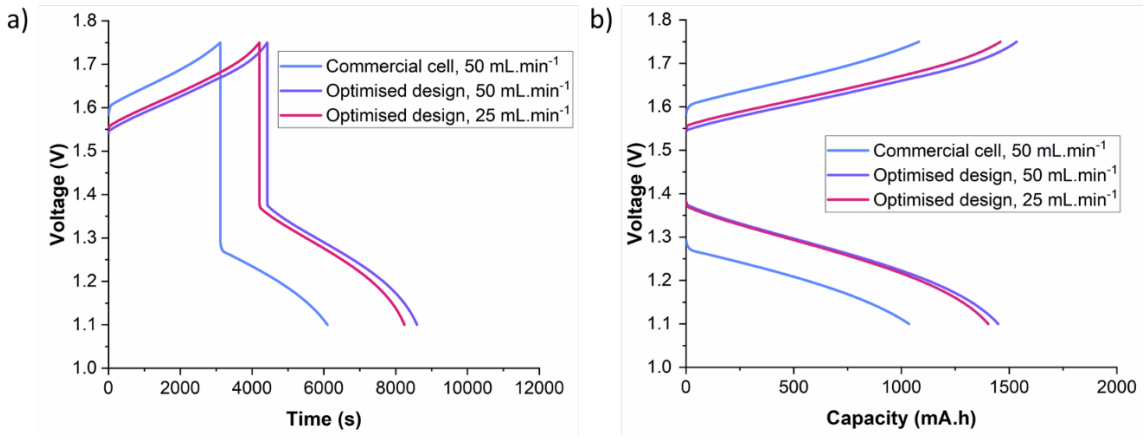

Figure S5. Charge-discharge results using set-up with 26% electrode compression in optimised cell at two different flow rates (50 mL min^{-1} and 25 mL min^{-1}) and commercial cell at 50 mL min^{-1}. (a) Voltage vs time plot and (b) voltage vs capacity plot

Cell cost analysis

This estimate includes: materials, electricity consumption, labour costs and 3D-printer costs associated with each cell manufactured. As this cost analysis is aimed at researchers manufacturing their own cells for lab use, it is assumed that the reader has lab space available to print and use the cell, and certain costs e.g. admin costs have been omitted.

The total cost (C_{total}) of the assembled flow cell as used in this work is given by:

$$C_{total} = C_{3D-print} + C_{sealing} + C_{endplates} \quad (4)$$

To calculate the cost of the 3D-printed flow frames, the following set of equations (5-9) developed by Li *et al.*[32], based on cost models from Hopkinson and Dickens[33] and Ruffo *et al.*[34], were used. The cost of the 3D-print components ($C_{3D-print}$) is given by:

$$C_{3D-print} = C_{machine} + C_{labour} + C_{material} + C_{energy} \quad (5)$$

The machine cost associated ($C_{machine}$) with each print is given by:

$$C_{machine} = \frac{p_{machine}}{t_{dep} \times e_u} \times t_{man} \quad (6)$$

where $p_{machine}$ is the purchase price of the 3D-printer, t_{dep} is the time for the 3D-printer to completely depreciate (which is taken to be 8 years[33]), e_u is the utilization rate of the printer (57 % for a printer running 100 hours per year, 50 weeks per year[32]) and t_{man} is the manufacturing time (~8.5 hours per half cell). Labour costs (C_{labour}) are calculated using[32]:

$$C_{labour} = C_{tecnician} \times t_{assist} \quad (7)$$

where $C_{tecnician}$ is the hourly salary an experienced lab technician at in the UK (approximated as \$20.87/h[35]) and t_{assist} is the time for assisting in the 3D-printing process (setup, removal of part from build plate, brim removal and cleaning). The total material cost $C_{material}$ is calculated using:

$$C_{material} = p_{material} \times \left(m_{material} + m_{support\ \&\ adhesion}\right) \quad (8)$$

where $p_{material}$ was the material price per unit gram, $m_{material}$ was the mass of the 3D-printed part and $m_{support\ \&\ adhesion}$, was the mass of supporting material and adhesion in grams. Material price was taken from the average price of ABS filaments purchased for use in this work (Ultimaker, FormFutura, and Verbatim ABS) resulting in a price of 0.056 \$ g^{-1}. The mass of two 3D-printed half cells is calculated by the slicing software as 134 g in total and the mass of the support and adhesion removed after printing for the 20 mm brim and O-ring support was 6 g. To account for failures during the printing process or accidental damage to components over time, an extra half-cell was normally printed for each design iteration. This was taken into account in the cost analysis, resulting in total print times of 22.65 hours and material usage of 201 g. The total energy cost was calculated as:

$$C_{energy} = P_{elec} \times C_{elec} \times t_{man} \quad (9)$$

where P_{elec} is the power consumed by the 3D-printer during the build and C_{elec} is the cost of energy per kWh. The value for C_{elec} was estimated using the average domestic energy price per kWh in the UK in 2020, which was 0.242 \$ kWh^{-1} [36] and the value for P_{elec} was estimated using the average power consumption of a number of low cost FDM 3D-printers of 0.0785 kW[37].

The costs of the non 3D-printed components used as endplates, ($C_{endplates}$) and for the sealing structure, ($C_{sealing}$) in the cell were calculated using:

$$C_{endplates} = A_{brass} \times C_{brass} + A_{graphite} \times C_{graphite} + C_{workshop} \quad (\mathbf{10})$$

where A_{brass} and $A_{graphite}$ are the area of brass and graphite used (including waste material) which was 165 cm^2 and 112 cm^2 respectively. C_{brass} and $C_{graphite}$ were the cost of the brass and graphite sheets per cm^2 at 0.083 \$ cm^{-2} and 0.034 \$ cm^{-2}, respectively, whilst $C_{workshop}$ was the cost to waterjet-cut the parts in the workshop at Queen's University Belfast, which was \$41.74. Lastly, the cost of the sealing structure ($C_{sealing}$) of the cell could be calculated:

$$C_{sealing} = A_{gasket} \times C_{gasket} + N_{O-ring} \times C_{O-ring} + C_{clamp} \quad (\mathbf{11})$$

where C_{O-ring} and N_{O-ring} represent the cost and number of O-rings. Each nitrile O-ring cost \$0.54 (Polymax) and each cell used four O-rings. The gasket cost per cm^2 (C_{gasket}) was 0.014 \$ cm^{-2} and the area of gasket used per cell (A_{gasket}) including waste was 332.5 cm^2. Finally, the Irwin clamp used (Irwin, RS Components) had a cost (C_{clamp}) of \$14.53.

CAD file Repository

Designs have been replicated in both Solidworks and Fusion 360 to provide parametric CAD models which facilitate customisation of the cell by users with 3D modelling/ CAD experience. Several variations of the cell design have been included to make the cells easier to use and print. Versions of the cell, with the optimised and unoptimised flow field designs have been made available as well as variations in the cell design including current collector guides, brims and a threaded inlet and outlet for a 1/8" NPT fitting. This variation was tested using a Polypropylene, Straight, Hose Barb to Threaded Adapter (Cole-Parmer) and PTFE thread seal tape, with no leaks occurring. Examples of these CAD files can be seen in Figure S5.

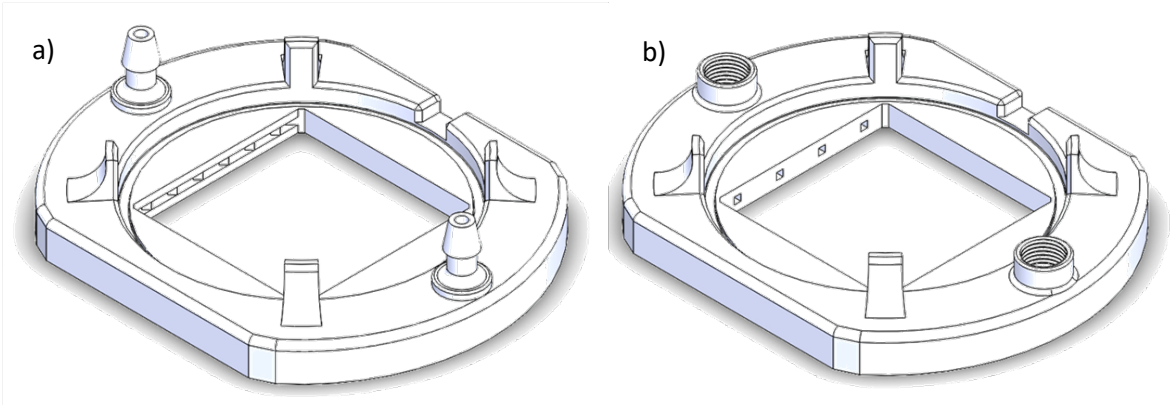

Figure S5. Examples of the variations of CAD files included. (a) File number 16. This design with an optimised manifold features 3D-printed nozzles and guides to make assist in cell assembly. (b) File number 6. This design has the unoptimised manifold and threaded in- and outlets for removable hose barb attachments.

The following files have been included in the Electronic Supplementary Information section*;

1. Original Cell with printed nozzles with brim; Solidworks, Fusion360, STL & STEP
2. Original Cell with printed nozzles no brim; Solidworks, Fusion360, STL & STEP

3. Original Cell with printed nozzles with brim; Solidworks, Fusion360, STL & STEP

4. Original Cell with printed nozzles no brim; Solidworks, Fusion360, STL & STEP

5. Original Cell with guides and screw in nozzles with brim; Solidworks, Fusion360, STL & STEP

6. Original Cell with guides and screw in nozzles no brim; Solidworks, Fusion360, STL & STEP

7. Original Cell with guides and printed nozzles with brim; Solidworks, Fusion360, STL & STEP

8. Original Cell with guides and printed nozzles no brim; Solidworks, Fusion360, STL & STEP

9. Optimised Cell with printed nozzles with brim; Solidworks, Fusion360, STL & STEP

10. Optimised Cell with printed nozzles no brim; Solidworks, Fusion360, STL & STEP

11. Optimised Cell with printed nozzles with brim; Solidworks, Fusion360, STL & STEP

12. Optimised Cell with printed nozzles no brim; Solidworks, Fusion360, STL & STEP

13. Optimised Cell with guides and screw in nozzles with brim; Solidworks, Fusion360, STL & STEP

14. Optimised Cell with guides and screw in nozzles no brim; Solidworks, Fusion360, STL & STEP

15. Optimised Cell with guides and printed nozzles with brim; Solidworks, Fusion360, STL & STEP

16. Optimised Cell with guides and printed nozzles no brim; Solidworks, Fusion360, STL & STEP

17. Drawing of Current Collector

18. Drawing of Gasket 1

19. Drawing of Gasket 2

20. Drawing of Graphite Plate

References

1. H. Sun, H. Takahashi, N. Nishiumi, Y. Kamada, K. Sato, K. Nedu, Y. Matsushima, A. Khosla, M. Kawakami, H. Furukawa, P. Stadler and T. Yoshida, *Journal of the Electrochemical Society*, 2019, **166**, B3125-B3130.
2. P. Ghimire, A. Bhattarai, R. Schweiss, G. Scherer, N. Wai and Q. Yan, *Applied Energy*, 2018, **230**, 974-982.
3. T. J. Davies and J. J. Tummino, *Journal of Carbon Research*, 2018, **4**.
4. J. Vrana, J. Charvat, P. Mazur, P. Belsky, J. Dundalek, J. Pocedic and J. Kosek, *Journal of Membrane Science*, 2018, **552**, 202-212.
5. P. Mazur, J. Mrlik, J. Benes, J. Pocedic, J. Vrana, J. Dundalek and J. Kosek, *Journal of Power Sources*, 2018, **380**, 105-114.
6. C. Armstrong and K. Toghill, *Journal of Power Sources*, 2017, **349**, 121-129.
7. D. Chen, M. Hickner, E. Agar and E. Kumbur, *Electrochemistry Communications*, 2013, **26**, 37-40.
8. D. Chen, M. Hickner, E. Agar and E. Kumbur, *Journal of Membrane Science*, 2013, **437**, 108-113.
9. K. Knehr, E. Agar, C. Dennison, A. Kalidindi and E. Kumbur, *Journal of the Electrochemical Society*, 2012, **159**, A1446-A1459.
10. C. Zhang, T. Zhao, Q. Xu, L. An and G. Zhao, *Applied Energy*, 2015, **155**, 349-353.
11. P. Leung, Q. Xu, T. Zhao, L. Zeng and C. Zhang, *Electrochimica Acta*, 2013, **105**, 584-592.
12. S. Kim, J. Yan, B. Schwenzer, J. Zhang, L. Li, J. Liu, Z. Yang and M. Hickner, *Electrochemistry Communications*, 2010, **12**, 1650-1653.
13. L. Li, S. Kim, W. Wang, M. Vijayakumar, Z. Nie, B. Chen, J. Zhang, G. Xia, J. Hu, G. Graff, J. Liu and Z. Yang, *Advanced Energy Materials*, 2011, **1**, 394-400.
14. W. Wang, Z. Nie, B. Chen, F. Chen, Q. Luo, X. Wei, G. Xia, M. Skyllas-Kazacos, L. Li and Z. Yang, *Advanced Energy Materials*, 2012, **2**, 487-493.
15. X. Wei, Z. Nie, Q. Luo, B. Li, B. Chen, K. Simmons, V. Sprenkle and W. Wang, *Advanced Energy Materials*, 2013, **3**, 1215-1220.
16. B. Li, M. Gu, Z. Nie, Y. Shao, Q. Luo, X. Wei, X. Li, J. Xiao, C. Wang, V. Sprenlde and W. Wang, *Nano Letters*, 2013, **13**, 1330-1335.
17. B. Jiang, L. Wu, L. Yu, X. Qiu and J. Xi, *Journal of Membrane Science*, 2016, **510**, 18-26.
18. Z. Li, W. Dai, L. Yu, L. Liu, J. Xi, X. Qiu and L. Chen, *Acs Applied Materials & Interfaces*, 2014, **6**, 18885-18893.
19. W. Dai, Y. Shen, Z. Li, L. Yu, J. Xi and X. Qiu, *Journal of Materials Chemistry a*, 2014, **2**, 12423-12432.
20. Z. Li, W. Dai, L. Yu, J. Xi, X. Qiu and L. Chen, *Journal of Power Sources*, 2014, **257**, 221-229.
21. S. Roe, C. Menictas and M. Skyllas-Kazacos, *Journal of the Electrochemical Society*, 2016, **163**, A5023-A5028.
22. T. Janoschka, N. Martin, U. Martin, C. Friebe, S. Morgenstern, H. Hiller, M. Hager and U. Schubert, *Nature*, 2015, **527**, 78-81.
23. T. Janoschka, N. Martin, M. Hager and U. Schubert, *Angewandte Chemie-International Edition*, 2016, **55**, 14425-14428.
24. X. Ma, H. Zhang and F. Xing, *Electrochimica Acta*, 2011, **58**, 238-246.
25. A. Shah, M. Watt-Smith and F. Walsh, *Electrochimica Acta*, 2008, **53**, 8087-8100.
26. D. You, H. Zhang and J. Chen, *Electrochimica Acta*, 2009, **54**, 6827-6836.
27. N. Gurieff, C. Cheung, V. Timchenko and C. Menictas, *Journal of Energy Storage*, 2019, **22**, 219-227.
28. K. Singh, *International Journal of Plastics Technology*, 2018, **22**, 177-184.
29. O. Carneiro, A. Silva and R. Gomes, *Materials & Design*, 2015, **83**, 768-776.
30. X. Ma, H. Zhang, C. Sun, Y. Zou and T. Zhang, *Journal of Power Sources*, 2012, **203**, 153-158.
31. D. Kim, S. Yoon, J. Lee and S. Kim, *Applied Energy*, 2018, **228**, 891-901.

32. Y. Li, B. Linke, H. Voet, B. Falk, R. Schmitt and M. Lam, *Cirp Journal of Manufacturing Science and Technology*, 2017, **16**, 1-11.
33. N. Hopkinson and P. Dickens, *Proceedings of the Institution of Mechanical Engineers Part C-Journal of Mechanical Engineering Science*, 2003, **217**, 31-39.
34. M. Ruffo, C. Tuck and R. Hague, *Proceedings of the Institution of Mechanical Engineers Part B-Journal of Engineering Manufacture*, 2006, **220**, 1417-1427.
35. National Careers Service, Laboratory technician job profile, https://nationalcareers.service.gov.uk/job-profiles/laboratory-technician).
36. E. I. S. GOV.UK Department for Business, *Statistical data set: Annual domestic energy bills*, 2021.
37. S. Walls, J. R. Corney and G. Vasantha, presented in part at the The 12 th International Conference on Manufacturing Research (ICMR2014), Southampton, 2014.